Title
Winkler Stiffness Intensity for Flexible Walls Retaining Inhomogeneous Soil

Authors
Durante, Maria Giovanna
Brandenberg, Scott J
Stewart, Jonathan P
et al.

Publication Date
2018

Peer reviewed

Winkler stiffness intensity for flexible walls retaining inhomogeneous soil

Maria Giovanna Durante, Ph.D.,[1] Scott J. Brandenberg, Ph.D., P.E., M.ASCE [2], Jonathan P. Stewart, Ph.D., P.E., F.ASCE [3], and George Mylonakis, Ph.D., M.ASCE[4]

[1]Department of Civil and Environmental Engineering, University of California, Los Angeles, 2270 Boelter Hall, Los Angeles, CA 90095-1593; e-mail: mgdurante@ucla.edu
[2]Department of Civil and Environmental Engineering, University of California, Los Angeles, 5731-D Boelter Hall, Los Angeles, CA 90095-1593; e-mail: sjbrandenberg@ucla.edu
[3]Department of Civil and Environmental Engineering, University of California, Los Angeles, 5731 Boelter Hall, Los Angeles, CA 90095-1593; e-mail: jstewart@seas.ucla.edu
[4]Department of Civil Engineering, University of Bristol, Bristol, UK; e-mail: g.mylonakis@bristol.ac.uk

ABSTRACT

The Winkler method is often adopted for the evaluation of the seismic response of retaining walls, and several closed form solutions in the literature present values for Winkler stiffness intensity (i.e., stiffness per unit area of wall) for certain simplified conditions. A common assumption in these solutions is that the wall is a rigid body. This paper presents an extensive parametric analysis of Winkler stiffness intensity for flexible elastic walls retaining inhomogeneous elastic soil. The finite element software framework OpenSees is used in the DesignSafe cyberinfrastructure to perform the analyses. The wall is cantilevered from a fixed base and its flexural stiffness is varied relative to the soil stiffness to cover a reasonable range. Pseudo-static excitation is applied to soil elements using horizontal body forces, producing variable wall and soil displacements. The Winkler stiffness intensity is then computed based on *(i)* the horizontal stress mobilized at the soil-wall interface, and *(ii)* the difference in displacement between the wall and the soil in the free-field. Results show that both wall flexibility and soil inhomogeneity significantly influence the Winkler stiffness intensity. In particular, the Winkler stiffness intensity for flexible walls can be up to three times greater than the values computed for rigid walls due to shear stresses mobilized at the wall-soil interface as the wall rotates due to flexure. This result indicates that Winkler stiffness intensity is not a fundamental soil parameter, and that values must be carefully selected to account for boundary conditions.

INTRODUCTION

The seismic response of retaining walls is traditionally analyzed using pseudo-static limit-equilibrium methods. The most popular method of this kind is the Mononobe-Okabe method, originally developed by Okabe (1924) and Mononobe and Matsuo (1929), and subsequently modified by several researchers (e.g. Seed and Whitman, 1970; Chen and Liu, 1990; Mylonakis et al., 2007; Xu et al., 2015). According to these methods, the dynamic increment of earth pressure is produced by an inertial force acting on an active wedge. A key conceptual shortcoming of these

approaches is that they fail to associate seismic earth pressure with relative wall-soil displacement, which is increasingly being recognized as the controlling demand parameter (e.g., Davis 2003, Brandenberg et al. 2015).

Another class of solutions involve elastodynamic analysis of an elastic soil layer resting on a rigid base and retained by a rigid or flexible wall (e.g., Wood 1973, Veletsos and Younan 1994a, 1994b, and 1997). These solutions are for wall resultant forces but do not specifically provide stiffness intensities. Although these solutions capture the relative wall-soil displacements that are produced by wave propagation and soil-structure interaction effects, the rigid base assumption produces strong resonance at the modal frequencies of the soil layer, and the seismic earth pressures can be very high at these frequencies. Soil generally does not rest on a rigid base in real systems, therefore these resonance effects are generally unrealistic.

Kloukinas et al. (2012) applied elastodynamic solutions for configurations similar to those considered in the classical solutions of Wood (1973) and Veletsos and Younan (1994a) (rigid walls retaining uniform elastic soil), specifically with the intent of deriving Winkler stiffness intensities. This was done to facilitate application of the Winkler method, which is widely used elsewhere in soil-structure interaction problems (e.g. Pais and Kausel, 1998; Gazetas 1991), to the wall-soil interaction problem. The stiffness intensities of Kloukinas et al. (2012) were used by Brandenberg et al. (2015) in formulating a solution for kinematic seismic earth pressure on retaining walls for general (rigid or flexible) base conditions. Subsequently, Brandenberg et al. (2017a) provide an approximate solution for Winkler stiffness intensity for rigid walls retaining vertically inhomogeneous elastic soil.

The objective of this paper is to extend the work of Brandenberg et al. (2017a) to study the combined effects of wall flexibility and soil inhomogeneity on Winkler stiffness intensity. The paper presents an extensive parametric analysis to compute Winkler stiffness intensity for various combinations of inhomogeneous soil deposits and flexible walls. All analyses are performed using the finite element (FE) software framework OpenSees (McKenna et al., 2001) running on the DesignSafe cyberinfrastructure (Rathje et al., 2017).

NUMERICAL SIMULATIONS SETUP

Figure 1 illustrates the problem under consideration. A flexible wall cantilevered from a fixed base supports vertically inhomogeneous soil overlying a rigid base. Although the rigid-base assumption for the soil results in unrealistic resonances in elastodynamic solutions, it is useful for deriving Winkler stiffness intensity values for use in simulations that utilize more realistic boundary conditions for the retained soil. Vertical inhomogeneity follows the form suggested by Rovithis et al. (2011), as defined by Equations 1 and 2, where G_0 is the shear modulus at the surface, G_H is the shear modulus at the base of the soil layer, n is an inhomogeneity factor, and $b=(V_0/V_H)^{1/n}$, and V_0 and V_H are the shear wave velocity at surface and at the base, respectively. Note that n=0 corresponds to homogeneous soil, and n=0.5 corresponds to a linear variation in shear modulus with depth.

$$G(z) = \rho V_r^2 \cdot f(z) \tag{1}$$

$$f(z) = \left[b + (1-b)\frac{z}{z_r}\right]^{2n} \tag{2}$$

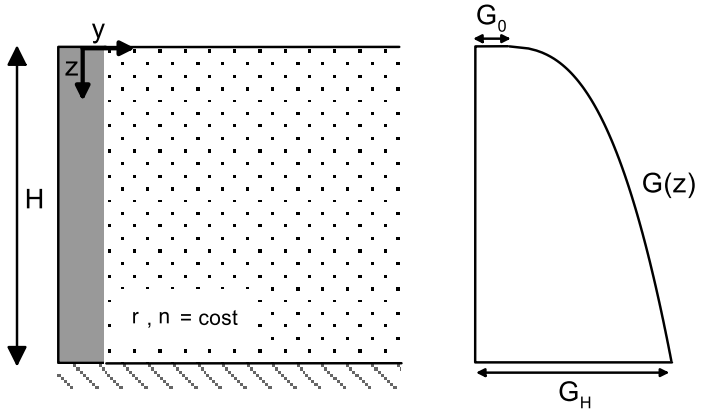

Figure 1. Fixed base wall retaining inhomogeneous soil.

The wall is modeled using elastic beam elements with constant flexural stiffness (*EI*) rigidly attached to the soil continuum immediately behind the wall. The stiffness of the wall relative to the soil is quantified using a dimensionless constant $(\beta H)^{-1}$, where β is defined by Equation 3, and $k^i_{yH,rig}$ indicates the stiffness intensity at the base of a rigid wall (Equation 4) following the solution by Brandenberg et al. (2017a). The stiffness of the wall relative to the soil increases with $(\beta H)^{-1}$ and the wall is essentially rigid for $(\beta H)^{-1}$ greater than two.

$$\beta = \sqrt[4]{\frac{k^i_{yH,rig}}{4EI}} \tag{3}$$

$$k^i_{yH,rig} = \frac{G_H}{H}\frac{2}{\sqrt{(1-\nu)(2-\nu)}}\left[1.057e^{-1.968(1-2n)-3.008b} + \frac{\pi}{2}\right] \tag{4}$$

A schematic of the two-dimensional FE model developed in OpenSees to analyze this problem is shown in Figure 2. The mesh is formed by four-node quadrilateral elements, and deformations of the mesh are driven by a static horizontal body force. This pseudostatic modeling approach does not incorporate the effect of frequency on stiffness intensity, as has been incorporated in previous elastodynamic solutions. The influence of frequency is important at high frequency where the wavelength of the vertically propagating shear wave is on the same order as the wall height. Static stiffness intensity is reasonably accurate when wavelength is significantly longer than wall height (Brandenberg et al. 2015). Soil inhomogeneity is incorporated by representing the layer as piecewise-constant in which each row of elements is assigned elastic properties computed at its mid-point in the vertical (*z*) direction.

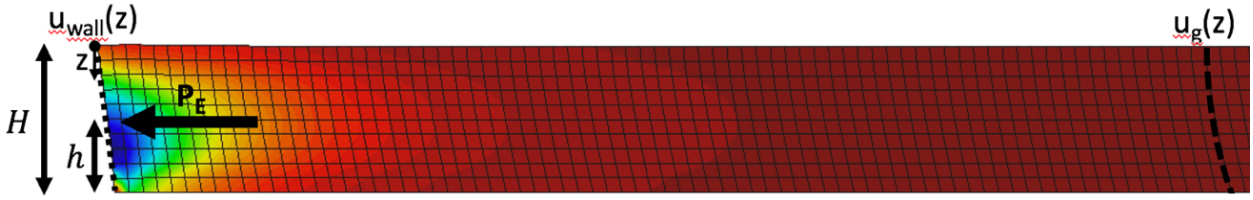

Figure 2. Numerical analysis approach.

The depth-variable static Winkler stiffness intensity, $k^i_{y,flex}(z)$, is computed based on mobilized horizontal earth pressures at the soil-wall interface and relative displacements between the wall (u_{wall}) and free-field soil (u_g). To simplify the solution, the depth variation of stiffness intensity is assumed to have the same form as the shear modulus [given by $f(z)$ in Equation 2].

$$k^i_{y,flex}(z) = k^i_{yH,flex} \cdot f(z) \tag{5}$$

where $k^i_{yH,flex}$ is stiffness intensity at the base of the wall, which is computed as:

$$k^i_{yH,flex} = \frac{\int_0^H \sigma_{yy}(z)dz}{\int_0^H \left(u_g(z) - u_{wall}(z)\right) \cdot f(z)dz} \tag{6}$$

where $\sigma_{yy}(z)$ is the horizontal pressure at the wall-soil interface at depth z.

The total length of the model is set to be 20 times the height of the wall, which was found to avoid the influence of the boundary effects on the wall-soil interaction. The free-field soil displacement (u_g) was obtained from a separate analysis in which the soil deposit is modeled as a shear beam without a structure. This "free-field" condition produces ground displacements that are essentially identical to those at the end of the model furthest from the wall, as indicated in Figure 2.

Parametric analysis. A parametric analysis was performed to study the influence of soil inhomogeneity and wall flexibility on Winkler stiffness intensity. The cyberinfrastructure DesignSafe (Rathje et al. 2017) is used to perform the analyses, which would have been computationally prohibitive to run on a personal computer. Based on Equation 1, a total of 81 shear wave velocity profiles were used in the parametric analysis obtained for G_0/G_H =0.1 to 0.9 in increments of 0.1 and n =0.05 to 0.45 in increments of 0.05. The homogenous soil deposit (G_0/G_H =1.0 and n =0.0) is also considered in the analysis. Figure 3 shows the complete set of dimensionless shear wave velocity profiles considered in the analysis. For each soil deposit considered, the flexural stiffness of the wall (EI) has been varied to cover a range of $(\beta H)^{-1}$ from 0.1 to 3, which covers the range of values anticipated for typical retaining structures. The combination of all the variables leads to a total of 7954 analyses.

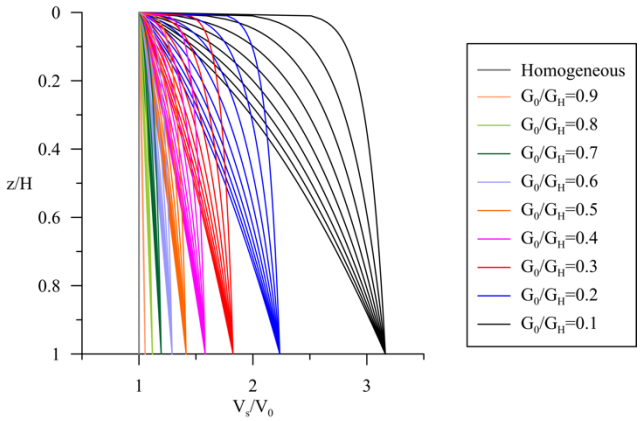

Figure 3. Shear wave velocity profiles used in the parametric analysis.

VERIFICATION FOR RIGID WALLS

Before proceeding with static Winkler stiffness intensity results for flexible walls, it is useful to first verify the outcome of the finite element solutions by comparing with published solutions for rigid walls retaining homogeneous and inhomogeneous soil from Kloukinas et al. (2012) and Brandenberg et al. (2017a) respectively. Results are presented in terms of kinematic force increment over the wall height, defined in Equation 7:

$$P_E = \int_0^H \sigma_{yy}(z)dz \tag{7}$$

Figure 4 shows the dimensionless kinematic force increment over the wall height, defined as $P_E/(k^i_{yH,rig}u_{g0}H)$ (Figure 4a) and the normalized position of the resultant force from the base of the wall, defined as *h/H* (Figure 4b) versus *n* for different values of G_0/G_H for a rigid cantilever wall. As inhomogeneity of the soil increases (i.e., as *n* increases and/or G_0/G_H decreases), the resultant force decreases. Furthermore, Figure 4b shows that increasing inhomogeneity shifts the position of the resultant downward.

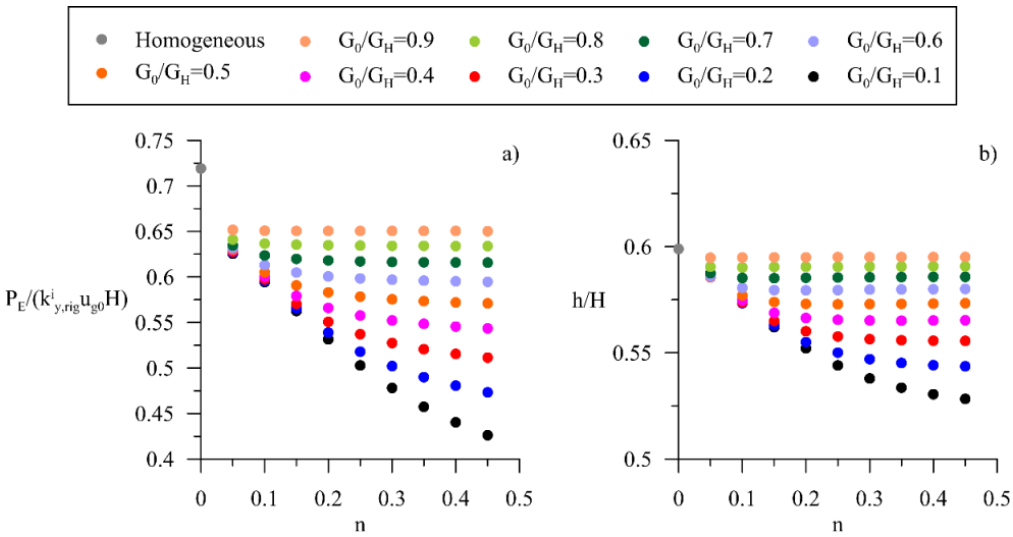

Figure 4. Dimensionless kinematic force increment (a) and its position (b) versus dimensionless inhomogeneity factor *n* for different values of G_0/G_H for rigid wall.

Figure 5a shows the dimensionless Winkler stiffness intensity, defined as $(k^i_{yH,rig}H)/G_H$, versus *n* for different values of G_0/G_H for a rigid cantilever wall. As soil inhomogeneity increases (i.e., as *n* increases and/or G_0/G_H decreases), the static Winkler stiffness intensity at the base of the wall increases. This trend is expected since the gradient of Winkler stiffness intensity with depth increases as soil inhomogeneity increases, rendering high stiffness intensity values at the base of the wall. Figure 5b shows the normalized difference between the analytical solutions formulated by Brandenberg et al. (2017a) for inhomogeneous soil and by Kloukinas et al. (2012) for homogeneous soil, and the numerical solutions. This normalized difference is defined as:

$$\Delta = \left(k^i_{yH,rig} - \frac{\int_0^H \sigma_{yy}(z)dz}{\int_0^H \left(u_g(z) - u_{wall}(z)\right) \cdot f(z)dz} \right) / k^i_{yH,rig} \tag{8}$$

The FE simulations predict values about 3% lower on average than Brandenberg et al. (2017a). Differences in the solutions may arise from mesh discretization errors in the finite element solutions, or due to assumptions in the approximate solution by Brandenberg et al. (2017a). Nevertheless, the discrepancy is small. Kloukinas et al. (2012) showed that Winkler stiffness intensity can differ by as much as 2% for parabolic compared with sinusoidal shape functions.

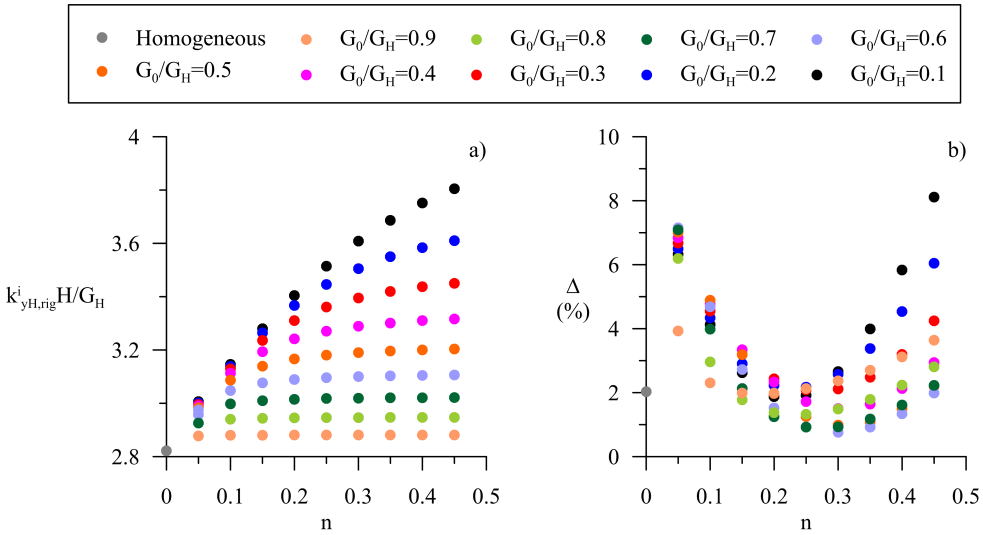

Figure 5. (a) Dimensionless Winkler stiffness intensity versus dimensionless inhomogeneity factor *n* for different values of G_0/G_H for rigid wall and (b) normalized difference (Δ) between the solutions.

RESULTS FOR FLEXIBLE WALLS

The dimensionless kinematic force increment and its position are presented versus the dimensionless wall stiffness parameter $(\beta H)^{-1}$ for different values of G_0/G_H and n in Figure 6. As the wall becomes more flexible, the dimensionless resultant force decreases, and shifts downward. The trends are approximately constant for $(\beta H)^{-1}$ values larger than about two, indicating that the wall is essentially rigid in this range. Figure 6 also shows comparison with the analytical solutions formulated by Younan and Veletsos (2000) and Brandenberg et al. (2017b) for flexible walls retaining homogeneous soil. The Younan and Veletsos (2000) approximate analytical solution applies for the seismic earth pressure acting on flexible walls retaining uniform soil under static conditions. They represent the wall flexibility using a dimensionless parameter d_w that is related to $(\beta H)^{-1}$ though Equation 9, where v_w is the Poisson ratio for the wall. The numerical method used in this paper produces the same response as the analytical solution proposed by Younan and Veletsos (2000). The Brandenberg et al. (2017b) solution uses the Kloukinas et al. (2012) expression for the Winkler stiffness intensity and it models the wall as a Euler-Bernoulli beam. Differences between the results presented here and those from the aforementioned previous analytical studies may arise from mesh discretization errors in the finite element solutions. As mentioned in the previous section, this can lead to differences as large as 2%.

$$d_w = \frac{4}{\pi}(\beta H)^4(1-\nu_w^2)\cdot\sqrt{(1-\nu)(2-\nu)} \tag{9}$$

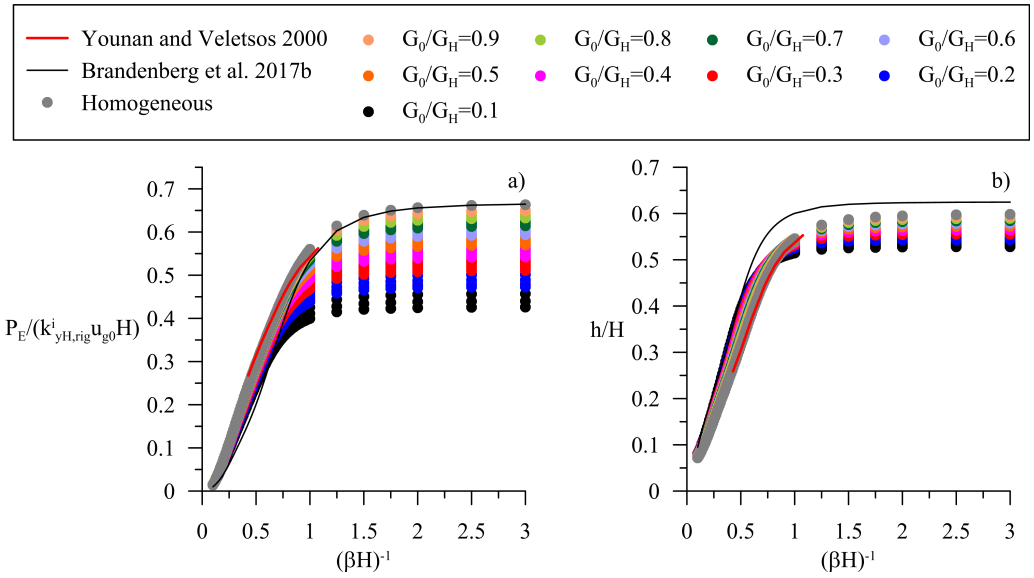

Figure 6. Dimensionless kinematic force increment (a) and its position (b) versus dimensionless Winkler parameter $(\beta H)^{-1}$ for flexible wall for different values of G_0/G_H and n (for each value of G_0/G_H, n increases from bottom to top).

The ratio of Winkler stiffness intensity at the base of the wall for a flexible wall relative to a rigid wall ($k^i_{yH,flex}/k^i_{yH,rig}$) is plotted versus $(\beta H)^{-1}$ for different values of G_0/G_H and n in Figure 7. The Winkler stiffness ratio does not depend significantly on soil inhomogeneity, but is very sensitive to wall flexibility. For very flexible walls ($(\beta H)^{-1} < 0.5$) the Winker stiffness intensity can be much higher than the value computed for a rigid wall (up to about three times). This increase is due to shear stresses mobilized at the wall-soil interface as the wall rotates due to flexure, and is consistent with observations for free-head versus fixed-head pile foundations (e.g., Syngros, 2004). The influence of shear stress on Winkler stiffness can be conceptualized using superposition principles. When the wall rotates away from the soil, shear stresses imposed on the soil at the interface act upward. These shear stresses, if imposed on their own, would cause the soil to deform away from the wall, in the opposite direction to the horizontal stresses. The resulting displacements are therefore less when the horizontal stresses and shear stresses act together. The hypothesis of rough interface assumed in the model using rigid connection between soil and wall elements likely influences this outcome, but simulations with smooth or partially rough interfaces have not yet been performed to more fully investigate this effect.

For ease of application, Equation 10 presents approximate expression for the static Winkler stiffness intensity ratio, developed through nonlinear least squares regression of data in Figure 7. The proposed equation provides a standard deviation of residuals equal to 0.02125 for the range of parameters considered.

$$\frac{k^i_{yH,flex}}{k^i_{yH,rig}} = 1 + exp\left[(\beta H)^{-1} \cdot \left(-5.24 + 3.26\frac{G_0}{G_H}n + 0.42\frac{G_0}{G_H} - 2.50n\right) + 0.99\right] \quad (10)$$

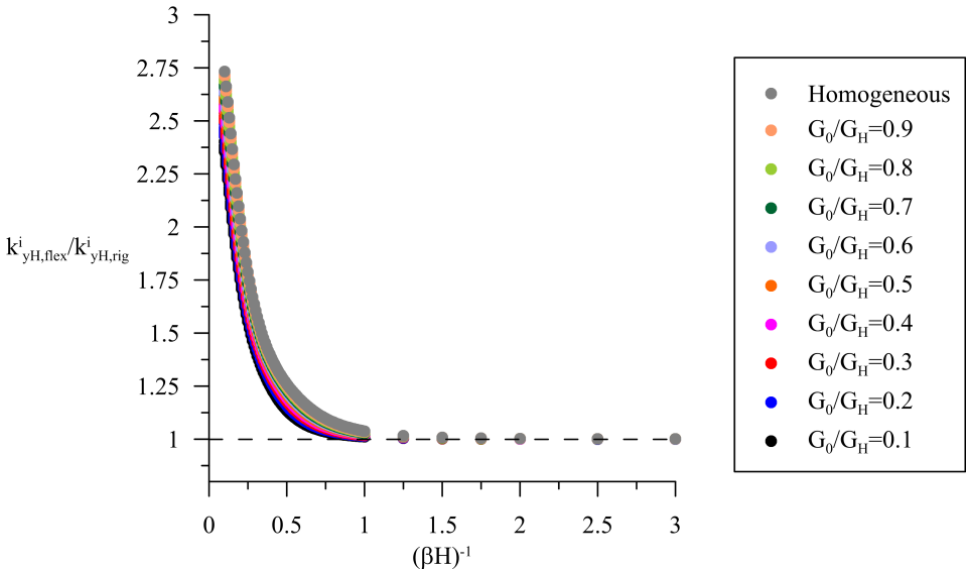

Figure 7. Dimensionless Winkler stiffness intensity for flexible wall versus dimensionless Winkler parameter $(\boldsymbol{\beta H})^{-1}$.

CONCLUSIONS

The paper presents an extensive parametric analysis of static Winkler stiffness intensity for flexible elastic walls retaining homogeneous and inhomogeneous soil. The finite element software framework OpenSees is used in the DesignSafe cyberinfrastructure to perform the analyses. The wall is cantilevered from a fixed base and its flexural stiffness is varied relative to the soil stiffness to cover a reasonable range of wall flexibility. The parametric analysis confirmed the following previously published trends:

- Soil inhomogeneity induces two main effects on the kinematic response of rigid cantilevered walls: *(i)* it reduces the kinematic force on rigid wall, and *(ii)* it moves the position of the resultant downward;
- Wall flexibility reduces the kinematic force acting on the wall and it shifts the resultant downward;
- For very flexible walls ($(\beta H)^{-1} < 0.5$), the combination of soil inhomogeneity and wall flexibility may increase the static Winkler stiffness intensity up to about three times greater than the values computed for rigid walls due to shear stresses mobilized by wall rotation.

While the above effects (i.e., the trends) had previously been recognized, the significance of this work is to quantify the above effects for a wide range of conditions, which is needed as SSI-based methods for seismic earth pressure analysis begin to make their way into practice. The expression in Equation 10, obtained by regressing the parametric study data, accomplishes this by quantifying the influence of wall flexibility on Winkler stiffness intensities.

ACKNOWLEDGMENTS

This research was funded by the California Department of Transportation through contract number 65A0582. Any opinions, findings, and conclusions or recommendations expressed in this material are those of the authors and do not necessarily reflect the views of the State of California or the California Department of Transportation.

REFERENCES

Brandenberg, SJ, JP Stewart, G Mylonakis (2017b). "Influence of wall flexibility on seismic earth pressures in vertically homogeneous soil," *Proc. Geo-Risk 2017: Impact of Spatial Variability, Probabilistic Site Characterization, and Geohazards*, Geotechnical Special Publication No. 285, Denver, CO.

Brandenberg, SJ, Mylonakis G, Stewart JP. (2015). "Kinematic framework for evaluating seismic earth pressures on retaining walls". *J Geotech Geoenviron Eng*: 1–10.

Brandenberg, SJ, Mylonakis G, Stewart JP. (2017a). "Approximate solution for seismic earth pressures on rigid walls retaining inhomogeneous elastic soil". *Soil Dyn Earthq Eng*; 97:468-477. https://doi.org/10.1016/j.soildyn.2017.03.028.

Chen, W.F., Liu, X.L. (1990). "Limit analysis in soil mechanics". Amsterdam, Netherlands: Elsevier.

Davis. C.A. (2003). "Lateral seismic pressures for design of rigid underground lifeline structures." *Sixth U.S. Conference and Workshop on Lifeline Earthquake Engineering (TCLEE)*.

Gazetas, G. (1991). "Foundation vibrations." Chapter 15, *Foundation engineering handbook*, 2nd Ed., H.-Y. Fang, ed., Chapman and Hall, New York.

Kloukinas, P., Langoussis, M., and Mylonakis, G. (2012). "Simple wave solution for seismic earth pressures on non-yielding walls." *J. Geotech. Geoenviron. Eng.*, 10.1061/(ASCE)GT.1943-5606.0000721, 1514–1519.

McKenna, F., and Fenves, G. L., (2001). "The OpenSees command language manual", version 2.5, http://opensees.berkeley.edu, *Pacific Earthquake Engineering Research Center*, University of California, Berkeley.

Mononobe, N., Matsuo, M. (1929). "On the determination of earth pressures during earthquakes". *Proc. World Eng. Congr. Engineering Society of Japan*, Tokyo, p. 179–87.

Mylonakis, G., Kloukinas, P., Papantonopoulos, C. (2007). "An alternative to the Mononobe-Okabe equation for seismic earth pressures". *Soil Dyn Earthq Eng*; 10:957–69.

Okabe, S. (1924). "General theory of earth pressure and seismic stability of retaining wall and dam". *J Jpn Soc Civ Eng*; 12:34–41.

Pais, A., and Kausel, E. (1988). "Approximate formulas for dynamic stiffnesses of rigid foundations." *Soil Dyn. Earthquake Eng.*, 7(4), 213–227.

Rathje, E., Dawson, C. Padgett, J.E., Pinelli, J.-P., Stanzione, D., Adair, A., Arduino, P., Brandenberg, S.J., Cockerill, T., Dey, C., Esteva, M., Haan, Jr., F.L., Hanlon, M., Kareem, A., Lowes, L., Mock, S., and Mosqueda, G. (2017). "DesignSafe: A New Cyberinfrastructure for Natural Hazards Engineering," *ASCE Natural Hazards Review*, doi:10.1061/(ASCE)NH.1527-6996.0000246.

Rovithis, EN, Parashakis H, Mylonakis GE. (2011). "1D harmonic response of layered inhomogeneous soil: analytical investigation". *Soil Dyn Earthq Eng*; 31:879–90. http://dx.doi.org/10.1016/j.soildyn.2011.01.007.

Seed, H. G., Whitman, R.V. (1970). "Design of earth retaining structures for dynamic loads". *ASCE Spec. Conf. Lateral Stress. Gr. Des. Earth Retaining Struct. American Society of Civil Engineers*, Reston; 1970, p. 103–47.

Syngros, C. (2004). "Seismic response of piles and pile-supported bridge piers evaluated through case histories". Ph.D. thesis, Civil Engineering Dept., City University of New York, NY.

Veletsos, A. S., and Younan, A. H. (1994a). "Dynamic soil pressures on rigid retaining walls." *Earthquake Eng. Struct. Dyn.*, 23(3), 275–301.

Veletsos, A., Younan, A. (1994b) “Dynamic Modeling and Response of Soil-Wall Systems.” *J Geotech Geoenviron Eng*: 120(12), 2155-2179.

Veletsos, A., Younan, A. (1997) “Dynamic Response of Cantilever Retaining Walls.” *J Geotech Geoenviron Eng*: 123(2), 161-172

Wood, J. H. (1973). “Earthquake induced soil pressures on structures.” *Rep. No. Earthquake Engineering Research Laboratory (EERL) 73-05*, California Institute of Technology, Pasadena, CA.

Xu, S-Y., Shamsabadi, A., Taciroglu E. (2015). “Evaluation of active and passive seismic earth pressures considering internal friction and cohesion”. *Soil Dyn Earthq Eng*, 70:30–47.

Younan, A.H., and Veletsos, A.S. (2000). “Dynamic response of flexible retaining walls.” *Earthquake Eng. And Struct. Dyn.* 29, 1815-1844.